

## Leapfrogging of two thick-cored vortex rings

This article has been downloaded from IOPscience. Please scroll down to see the full text article.

2013 Fluid Dyn. Res. 45 035503

(<http://iopscience.iop.org/1873-7005/45/3/035503>)

View [the table of contents for this issue](#), or go to the [journal homepage](#) for more

Download details:

IP Address: 205.175.97.252

The article was downloaded on 10/09/2013 at 20:09

Please note that [terms and conditions apply](#).

# Leapfrogging of two thick-cored vortex rings

Jagannadha Satti and Jifeng Peng

Department of Mechanical Engineering, University of Alaska Fairbanks, PO Box 755905,  
Fairbanks, AK 99775, USA

E-mail: [jpeng@alaska.edu](mailto:jpeng@alaska.edu)

Received 6 June 2012, in final form 24 March 2013

Published 14 May 2013

Online at [stacks.iop.org/FDR/45/035503](http://stacks.iop.org/FDR/45/035503)

Communicated by L Mydlarski

## Abstract

Leapfrogging of two vortex rings of thick cores is studied in laboratory experiments. Quantitative flow measurements show that, during leapfrogging, vorticity at the outer portion of the two cores diffuses together. However, the two cores remain clearly differentiable with distinct peaks. Vortex circulation decreases at a faster rate when the two rings are aligned radially and the passing ring is closer to axis touching due to vorticity cancellation. When two consecutive passages occur, vorticity cancellation is reduced in the second passage because the passing ring is further away from axis touching compared with that in the first passage. The study also finds that when the interval between generations of two rings is small, the front ring strongly influences the formation of the rear ring, whose core has an elongated tail of vorticity on its formation. The rear ring later sheds vorticity, whose amount increases with a smaller initial separation. The shedded vorticity, when strong enough, counters the effect of the front ring and prevents leapfrogging.

(Some figures may appear in color only in the online journal)

## 1. Introduction

Vortex rings are axisymmetric vortices that translate along their axis of symmetry. The phenomenon of leapfrogging, or slip-through, of a pair of co-axial co-rotating vortex rings has attracted great interest from researchers in fluid mechanics. A theoretical description was first introduced by Helmholtz (1858), and later discussed in many textbooks (e.g. Lamb 1895, Batchelor 1967). Due to mutual interaction, the toroidal radius of the front ring increases while the radius of the rear ring decreases. When the radius of the front ring becomes larger than that of the rear ring, the motion of the front ring is decelerated and that of the rear ring is accelerated. Under favorable conditions, the rear ring may catch up with the front ring, and be drawn through its center and emerge ahead of the front ring. Thereafter two

vortex rings reverse roles and they repeat the leapfrogging. An ideal example is two initially identical circular vortex filaments with infinitesimal core size in an ideal fluid, which are able to generate an infinite number of consecutive leapfrogging passages. Leapfrogging and vortex interaction, in general, are widely considered as enhancing transport and mixing in fluid flows.

Compared with the simple theoretical description of leapfrogging, it is much more difficult to produce leapfrogging in laboratory experiments where rings have finite core sizes and the fluid is viscous. Early efforts by Maxworthy (1972) and Oshima *et al* (1975), in which the vortex rings had Reynolds number ( $Re = UD/\nu$ , where  $U$  is the initial velocity of translation of the vortex ring,  $D$  the nozzle diameter and  $\nu$  the kinematic viscosity of liquid) less than 600, failed to observe leapfrogging and found that two rings merged into one. The first successful leapfrogging produced in a laboratory experiment was reported by Yamada and Matsui (1978), in which the vortex rings had  $Re = 1600$ . The success of leapfrogging at a larger  $Re$  was partially attributed by Shariff *et al* (1989) to vortex cores of smaller size. Using ideal flow assumptions and contour dynamics simulation, Shariff *et al* (1989) demonstrated that the core of the rear ring is subject to strain induced by the front ring. For rings with thin cores, the cores hardly distort and remain slender during leapfrogging. For rings with thick cores, the interaction could be strong enough for the rear ring to experience significant deformation to prevent leapfrogging.

Other than the  $Re$  of vortex rings, the initial spacing between two rings is also considered important. Apparently, if the spatial separation of two rings is too large, the interaction is small and the rear ring is not able to catch up with the front ring. On the other hand, there is also a lower limit for the spacing between two rings for successful leapfrogging. Oshima (1978) found that if the spatial separation between two rings is too small, the rings are not distinct initially and there is no leapfrogging. The study by Lim (1997) contested that the time interval between two ring generations must be sufficiently large compared with the time required for vortex sheet rolling up in ring formation. However, the exact effect of the front ring on the formation of the rear ring which prevents leapfrogging is still unclear.

In all the above-mentioned experimental studies, vortex rings were visualized by smoke or dye. These studies provided a better understanding on conditions on which leapfrogging can successfully occur. However, as pointed out by Maxworthy (1979) when questioning the interpretations in Yamada and Matsui (1978), because smoke and dye have very large Schmidt numbers (ratio of momentum to tracer diffusivity), they do not strictly track vorticity in these leapfrogging experiments and their motion does not strictly reflect that of vortex vorticity. Therefore, it is impossible to obtain precise information regarding core shapes and positions from smoke or dye visualization, especially when rings have thick cores (Maxworthy 1979). Quantitative flow measurements are necessary to fully understand the evolution of vortex rings in leapfrogging, and though they have become a standard in experimental fluid dynamics, they were used in few studies on this subject. One exception was a recent study by Mariani and Kontis (2010), in which vorticity fields were measured on rings with very high  $Re$  and thin cores generated by a diaphragm-based shock tube in the supersonic regime. In their study, no core motion or circulation was investigated.

Due to the fact that most theoretical and numerical studies were limited to inviscid assumptions and most experimental studies only provided qualitative flow measurements (a review is provided by Meleshko 2010), many questions remain for the leapfrogging process in real flow. One particular question is the leapfrogging process of rings of thick cores. Maxworthy (1979) speculated that the vorticity of the two rings might diffuse together. Shariff *et al* (1989) suggested the real case as a combination of their inviscid calculation and Maxworthy's diffusion arguments. In this study, we investigate the leapfrogging process of two rings of thick cores from quantitative flow measurements. We aim to determine the

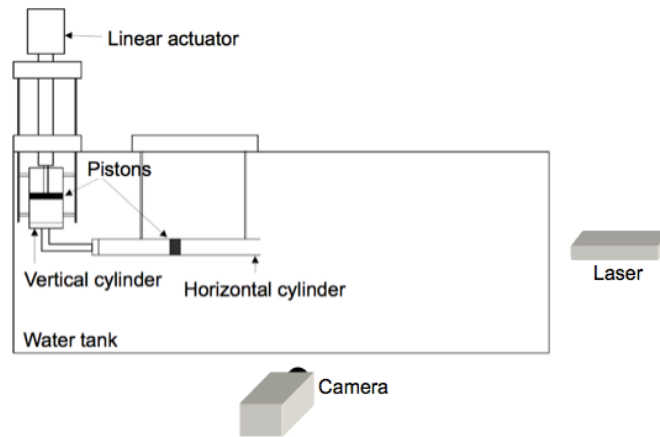


Figure 1. Schematic view of the piston-cylinder apparatus and DPIV.

evolution of vortex rings in terms of vorticity distribution, core motion and deformation, and vortex circulation. Also, the reason that leapfrogging is deterred at small intervals between ring formations is explored through vorticity measurements.

## 2. Method

In our experiments, vortex rings are generated by a classical piston-cylinder apparatus (figure 1). The piston inside a vertically placed cylinder is attached to a linear actuator. Another cylinder is placed horizontally, and together with a piston inside it, acts as the vortex ring generator. The vertical and horizontal cylinders are connected using rigid tubing fully filled with water. The system is submerged in a  $1.5 \times 0.6 \times 0.6$  m clear acrylic water tank during experiments. When the linear actuator extends its arm and drives the piston in the vertical cylinder, it also drives the piston in the horizontal cylinder through the water in the tubing to generate vortex rings. The linear actuator is able to drive the piston at a prescribed motion through a custom-designed control program on a PC. The two cylinders in the system have different sizes. The vertical cylinder has a diameter of  $D_0 = 10$  cm and the horizontal cylinder has a diameter of  $D = 5$  cm, with its outer contour wedge shaped with a tip angle of  $15^\circ$ . While the maximal operational translation velocity of the linear actuator is  $5 \text{ cm s}^{-1}$ , the arrangement allows the piston inside the horizontal cylinder to move at four times the speed to generate vortex rings of Reynolds numbers up to  $10^4$ , based on nozzle diameter and piston velocity.

In experiments, the piston velocity profiles used to generate consecutive vortex rings consist of two identical near-trapezoidal pulses. The piston velocity profile averaged over five measurements is shown in figure 2. Each pulse of the piston motion has a stroke-distance to nozzle-diameter ratio of  $L/D = 1.5$ , a pulse duration of  $t_p = 1.2$  s, an average velocity of  $U_p = 6.25 \text{ cm s}^{-1}$  and a peak velocity of  $12.15 \text{ cm s}^{-1}$ . Experiments are performed with various values of the time interval between two pulses  $\tau$ , which is quantified by the non-dimensional parameter  $\tau^* = \tau/t_p$ .

The flow on the symmetry plane is measured using digital particle image velocimetry (DPIV). A CCD camera with a resolution of  $1920 \times 1080$  pixels and a 30 Hz frame rate records the motion of particles, which are suspended in the flow and illuminated by a sheet of

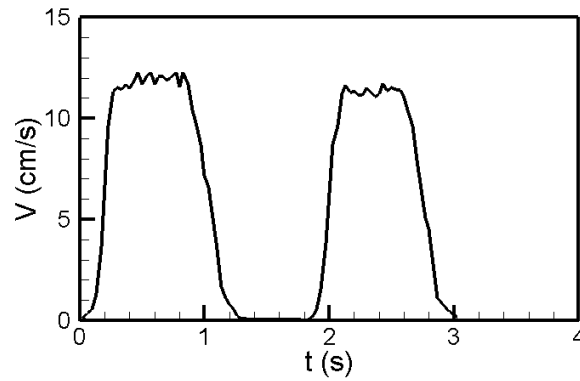


**Figure 2.** Piston velocity profile for generating two vortex rings.

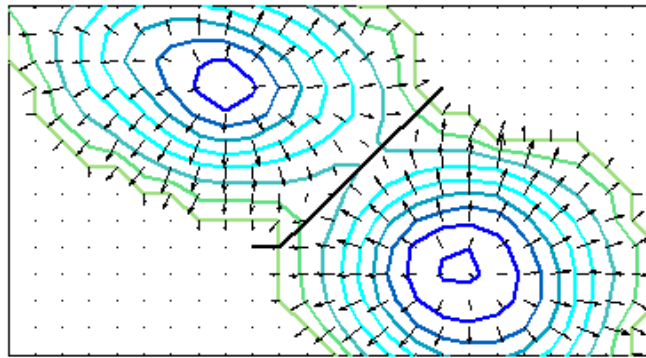


**Figure 3.** Vorticity contour of two nearby vortex cores and the boundary separating them. Black line: the boundary between two vortex cores, defined as the path from the saddle point with the steepest descent/ascent to background vorticity. Vectors: gradient of vorticity.

laser light with a thickness of 2 mm. The particles are silver-coated neutrally buoyant hollow glass beads with an average diameter of  $14\ \mu\text{m}$  and a standard deviation of  $5\ \mu\text{m}$ . Sequences of images of particle motion are analyzed to determine the two-dimensional velocity vector field of flow using an algorithm similar to that in Willert and Gharib (1991). A correlation-window size of  $64 \times 64$  pixels and a moving average step size of  $16 \times 16$  pixels are used in the analysis and flow velocity vector fields are generated on a  $120 \times 67$  grid with a typical field of view of  $28 \times 16$  cm and a spatial resolution of  $0.25 \times 0.25$  cm. From the velocity field, flow vorticity is calculated using the central difference scheme. The uncertainty in the velocity and vorticity measurement is 1 and 3%, respectively (Weigand and Gharib 1994).

The vortex core is considered as bounded by the contour line of 0.05 peak vorticity value. The effective core diameter is calculated from the cross-section area of the vortex core by  $\delta_0 = (4A/\pi)^{1/2}$ . The ring circulation is calculated by the area integration of vorticity within the vortex core. When two vortex cores move close, the boundary separating them is defined as the path on the vorticity contour from the saddle point with the steepest descent/ascent to background vorticity (figure 3). For simplicity, in practice the line linking all points where contour lines from two vortex cores connect is used to separate the two cores. The discrepancy in circulation calculation is negligible. The core peak vorticity location is determined with sub-grid accuracy by the local fit of a two-dimensional second-order polynomial function.

The front vortex ring, which can be considered as an isolated ring during its formation, has initial toroidal diameter  $d_0 = 6.87$  cm, area-effective core diameter  $\delta_0 = 2.81$  cm and translational speed  $U_0 = 2.25$  cm s<sup>-1</sup>, measured at the completion of the first piston pulse. To be consistent with previous studies on vortex ring leapfrogging, the Reynolds number is defined based on ring diameter and translational speed  $Re = d_0 U_0 / \nu = 1546$ , where  $\nu$  is water kinematic viscosity. The rings have an initial core radius to toroidal radius ratio  $\alpha = \delta_0 / d_0 = 0.41$ , and are considered to be of thick cores herein.

### 3. Results

Leapfrogging is observed in experiments for various values of time interval  $\tau^*$  for  $L/D = 1.5$ . A special case is for  $\tau^* = 0.5$ , when two passages are completed. Figure 4 shows the flow vorticity fields at a sequence of time instants, denoted by the non-dimensional time  $t^* = t/t_p$ . The background vorticity below 0.05 of peak value is neglected. Time  $t^* = 0$  represents when the piston starts the first pulse. At  $t^* = 2.5$ , the piston has completed two pulses and two rings are generated. The counter-rotating stopping vortex at the nozzle exit is also visible at this frame. The front ring generated from the first pulse has a circular shape, similar to that of an isolated ring. However, due to the influence of the front ring on its formation process, the rear ring generated during the second pulse has an elongated tail. The vorticity in the tail is later shed from the rear ring at  $t^* = 3.08$  and trails behind it. The core of the passing ring is deformed to an elliptical shape as it moves closer to the axis, because of the higher shear in the flow induced by the outer ring. At  $t^* = 3.39$ , the rear ring leaps ahead of the front ring. The first leapfrogging process is complete at  $t^* = 4.67$ , when the two cores are located in parallel in the axial direction. Two rings switch roles and repeat the process during the second passage, which completes at  $t^* = 6.97$ . The cores remain clearly differentiable with two distinct peaks during the entire leapfrogging process. The two rings eventually merge into one during the attempt of the third leapfrogging ( $t^* = 8.83$ ).

The temporal evolutions of circulations of the two rings for  $t^* = 0.3, 0.5$  and  $0.9$  are shown in figure 5. All plots start at piston motion in the first pulse ( $t^* = 0$ ). Spatial core separations, measured by the differences in core peak locations in the axial direction  $\Delta x = x_2 - x_1$  and the radial direction  $\Delta r = r_2 - r_1$ , respectively (indices denote the order of rings generated), are also shown in figure 5. Marked by vertical dashed lines in the plots are time instants at  $\Delta x = 0$ , when the rear ring is about to pass the front ring; and at  $\Delta r = 0$ , when a leapfrogging process is just complete. For  $\tau^* = 0.3$  (figure 5(a)), the leapfrogging is not complete before the two rings merge (when vorticity peaks of the two rings are no longer distinguishable and the measurements of  $\Delta x$  and  $\Delta r$  stop). For  $\tau^* = 0.5$  (figure 5(b)), two complete passages are observed, as  $\Delta x$  and  $\Delta r$  change sign twice. Only one complete leapfrogging process is observed for  $\tau^* = 0.9$  (figure 5(c)).

The evolution of circulation in ring formation is similar for all three cases. The circulation of the first ring  $\Gamma_1$  increases during its formation and then stays stable as the second ring is generated. At the completion of its formation, the circulation of the second ring  $\Gamma_2$  approximately equals  $\Gamma_1$ . The evolution of ring circulations during leapfrogging varies due to differences in ring interaction. For  $\tau^* = 0.3$  (figure 5(a)), there is a significant decrease in circulation for the second ring at  $t^* = 2.55$ , indicating a strong shedding of vorticity into the wake. As the second ring attempts leapfrogging,  $\Gamma_2$  decreases fast while there is a small increase in  $\Gamma_1$ . The small increase in  $\Gamma_1$  is mostly due to the diffusion of vorticity from  $\Gamma_2$ . The fast decrease in  $\Gamma_2$  indicates that only a small portion in the decrease of  $\Gamma_2$  can be attributed to an increase in  $\Gamma_1$ , whereas a larger portion is due to vorticity cancellation when the second ring becomes axis touching. The axial separation  $\Delta x$  changes sign at  $t^* = 2.50$  when the

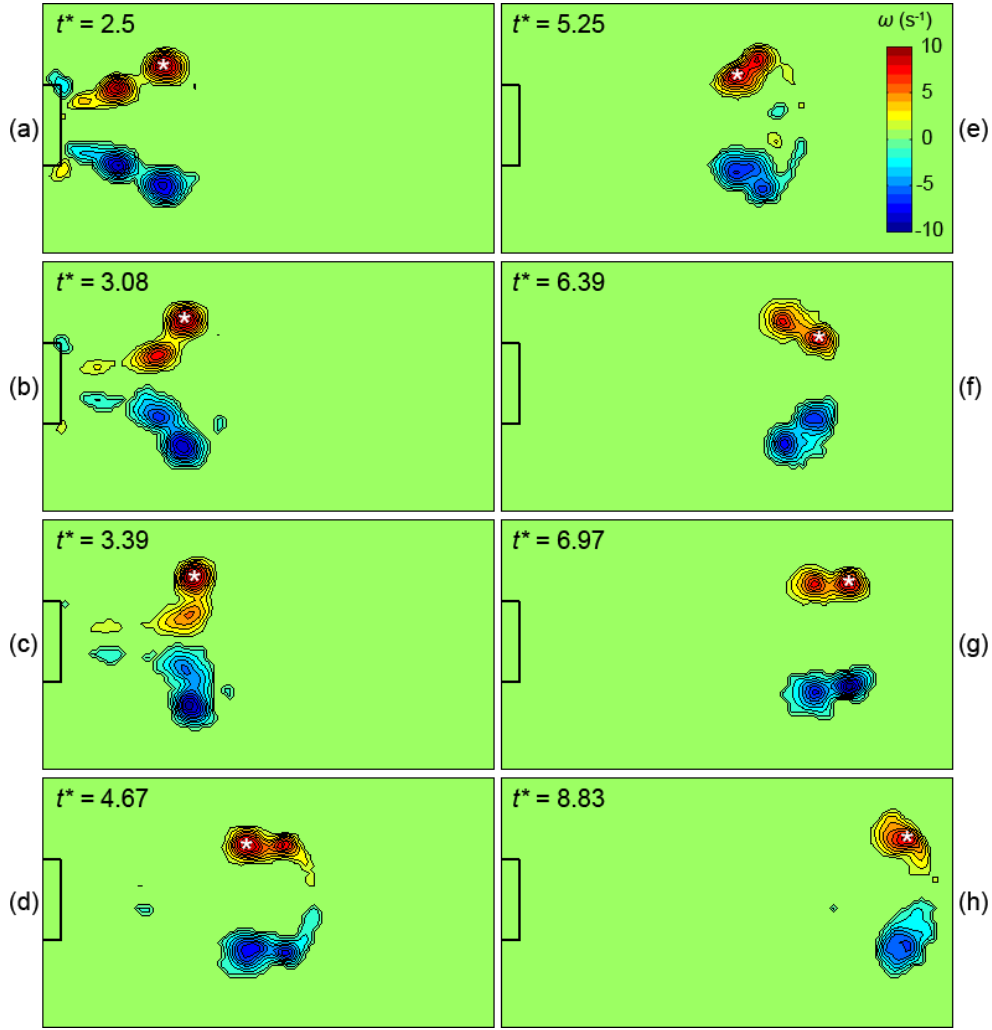


**Figure 4.** Evolution of vorticity fields during leapfrogging of two vortex rings formed with  $L/D = 1.5$  and  $\tau^* = 0.5$ , showing on eight frames starting from when the second ring is formed ( $t^* = 2.5$ ) to when two rings eventually merge into one ( $t^* = 8.83$ ) after two complete passages. The first ring generated is marked by the symbol '\*' at the top core center. The cylinder exit is also shown as the rectangle. The low level of background vorticity below a threshold of 0.05 peak value is neglected. (a)  $t^* = 2.5$ , (b)  $t^* = 3.08$ , (c)  $t^* = 3.39$ , (d)  $t^* = 4.67$ , (e)  $t^* = 5.25$ , (f)  $t^* = 6.39$ , (g)  $t^* = 6.97$  and (h)  $t^* = 8.83$ .

second ring passes the first ring. However, two rings do not complete the leapfrogging and merge at  $t^* = 2.83$ , as  $\Delta r$  is negative through the process. For  $\tau^* = 0.5$  (figure 5(b)),  $\Gamma_2$  keeps relatively stable for a short period before dropping at  $t^* = 3.08$  due to the shedding of vorticity. The vorticity shedding is also shown in the vorticity plot of figure 4(b). The drop in  $\Gamma_2$  due to vorticity shedding is much smaller compared with that in  $\tau^* = 0.3$ . As the second ring attempts leapfrogging,  $\Gamma_2$  decreases largely due to vorticity cancellation when the passing ring becomes axis touching. The first leapfrogging process completes at  $t^* = 4.67$ , when  $\Delta r$  changes sign. During the second leapfrogging process, the rear ring circulation

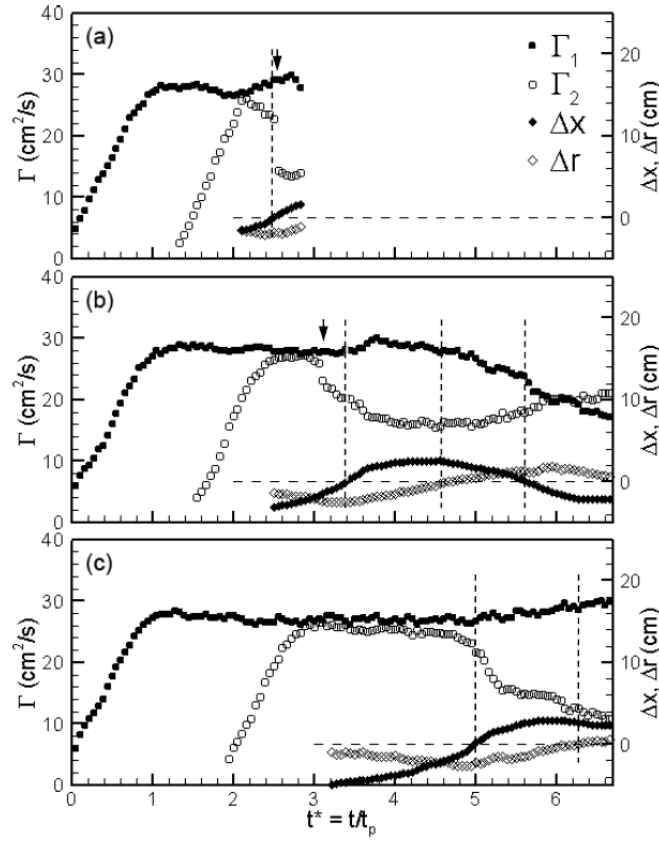


**Figure 5.** Temporal evolution of circulation of the first ring ( $\Gamma_1$ , filled circles) and the second ring generated ( $\Gamma_2$ , open circles) for  $L/D = 1.5$  and  $\tau^*$  equal to (a) 0.3, (b) 0.5 and (c) 0.9. Arrows show the instants when vorticity is shed from the rear ring. Also shown are  $\Delta x$  (filled diamonds) and  $\Delta r$  (open diamonds), the separations between peak vorticity locations of two cores in axial and radial directions, plotted to the vertical axis on the right. Vertical dashed lines indicate time instants when  $\Delta x$  or  $\Delta r$  are 0. Measurements of  $\Gamma$  begin at  $t^* = 0$ , when the piston starts the first pulse. All plots have the same scale in  $t^*$ .

decreases, whereas the front ring circulation increases, similar to the first leapfrogging. For  $\tau^* = 0.9$  (figure 5(c)),  $\Gamma_2$  enters a plateau after ring formation during which the second ring moves closer to the first ring. There is no vorticity shedding because, at larger separation, the first ring affects the formation of the second ring less.  $\Gamma_2$  begins to decrease considerably during the passage due to vorticity cancellation when axis touching. The leapfrogging process completes at  $t^* = 6.28$ , as  $\Delta r$  changes sign.

In all leapfrogging processes plotted in figure 5, including the attempted passage in  $\tau^* = 0.3$ , there is a sharp contrast between the circulations of the passing ring and the passed ring. The circulation of the passing ring (i.e.  $\Gamma_2$  for all passages except for  $\Gamma_1$  in the second passage for  $\tau^* = 0.5$ ) decreases significantly, whereas the circulation of the passed ring (i.e.  $\Gamma_1$  for all passages except for  $\Gamma_2$  in the second passage for  $\tau^* = 0.5$ ) experiences a small increase. For the passing ring, its circulation decreases faster around  $\Delta x = 0$ , compared with a much slower decrease around  $\Delta r = 0$ . This is consistent in the first leapfrogging process in both  $\tau^* = 0.5$  and 0.9 (figures 5(b) and (c)). The stronger decrease near  $\Delta x = 0$  is because at



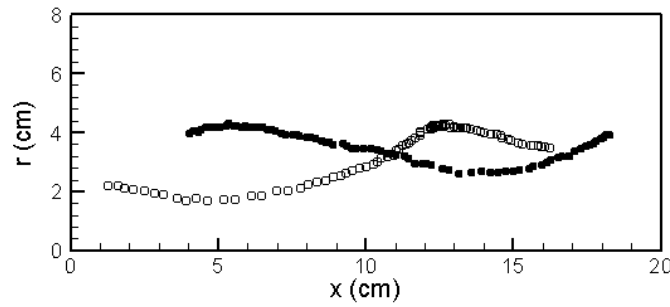


**Figure 6.** Trajectories of the core center for the first ring (filled circles) and the second ring (open circles) during two leapfrogging processes for  $\tau^* = 0.5$ . During the second passage, the core of the passing ring is further away from axis touching than that in the first passage. The axis is at  $r = 0$ .

this spatial configuration, the passing ring has a smaller toroidal radius and its core is closer to axis touching and thus is subject to more vorticity cancellation (figure 4(c)). During the second leapfrogging process for  $\tau^* = 0.5$  (figure 5(b)), however, the decrease near  $\Delta x = 0$  is much smaller compared with that in the first passage, indicating that vorticity cancellation for the passing ring during the second passage is not as significant. This can be explained by the differences in ring trajectories in the two passages, which is shown in figure 6. During the first passage, the passing ring that leaps to the front is close to the axis; thus it loses a significant portion of its circulation due to vorticity cancellation. Therefore, at the beginning of the second passage, the front ring is not as strong as the rear ring (figure 4(d)). Thus, the front ring induces a smaller shear and the rear ring experiences a smaller contraction in its toroidal radius during the second passage. Compared with that in the first passage, the core of the passing ring in the second passage is further away from the axis and has similar size; thus it is subject to less vorticity cancellation and its circulation decreases by a smaller amount.

#### 4. Conclusion and discussions

Compared with the theoretical description of leapfrogging of two circular vortex filaments, there are some new features for the leapfrogging of two thick-cored vortex rings. Because of the shear induced by the front ring, the core of the rear ring experiences deformation, or elongation in particular. When the interval between the two rings is small, the interaction between the two rings is strong and vorticity shedding from the elongated rear ring may occur. During leapfrogging, when the ring core radius to the ring toroidal radius is large, the passing ring is close to axis touching and thus its circulation decreases due to vorticity cancellation. In consecutive leapfrogging processes, after vorticity cancellation and circulation decrease for the passing ring in the first leapfrogging, the front ring in the second leapfrogging would have smaller circulation and thus induce a smaller shear. Therefore the rear ring would be subject to less contraction in the toroidal radius and less vorticity cancellation because the core is further away from axis touching.

The study provided a new, clear explanation of why leapfrogging is difficult at small intervals between the two rings. The interval between the two vortex rings has a significant effect on the behavior of the leapfrogging process because strong vortex shedding from the rear ring at small ring intervals could prevent leapfrogging. The differences in ring circulation shown in figure 5 are due to the different ring intervals as the piston pulses are the same. At a smaller interval  $\tau^* = 0.3$ , the two rings merge into one without completion of leapfrogging,

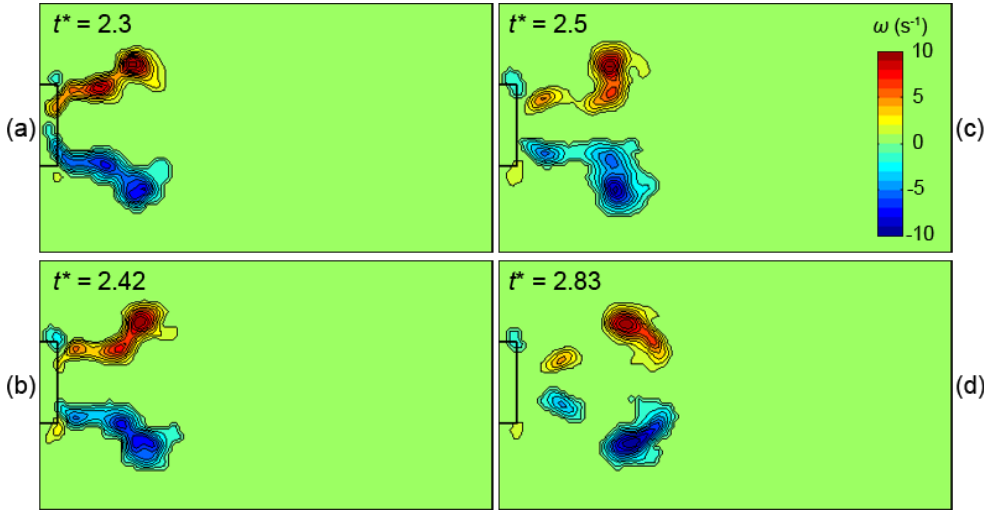


**Figure 7.** Evolution of vorticity fields during leapfrogging of two vortex rings formed with  $L/D = 1.5$  and  $\tau^* = 0.3$ . The vorticity shedding is much larger than that in  $\tau^* = 0.5$ . (a)  $t^* = 2.3$ , (b)  $t^* = 2.42$ , (c)  $t^* = 2.5$  and (d)  $t^* = 2.83$ .

whereas at larger intervals  $\tau^* = 0.5$  and  $0.9$ , there is complete leapfrogging. The difficulty of leapfrogging at smaller ring intervals is not directly due to the close proximity of the two cores because, even for two rings initially clearly separated and able to leapfrog, they become close to each other during leapfrogging (figure 4(b)). Rather, it can be attributed to the strong vortex ring interaction and the large shedding of vorticity from the rear ring. Figure 7 shows the vorticity fields for  $\tau^* = 0.3$ . Apparently, with a smaller  $\tau^*$ , the influence of the front ring on the formation of the rear ring is more significant. Compared with  $\tau^* = 0.5$  (figure 4), the rear ring generated during the second pulse has an elongated tail with stronger vorticity at the completion of ring formation. The trailing vortex shed later from the rear ring is also much larger in circulation. While the front ring induces a velocity that causes the rear ring to contract in size, the shed vorticity, of the same sign and trailing behind, induces a radial velocity component pointing away from the axis at the rear ring and causes it to expand radially and move toward the front ring. At  $\Delta x = 0$ , when the rear ring leaps ahead of the front ring, the separation in the radial direction is  $\Delta r = 1.81$  cm for  $\tau^* = 0.3$  and  $\Delta r = 2.56$  cm in the first leapfrogging for  $\tau^* = 0.5$  (figures 5(a) and (b)). When strong enough, the trailing vorticity would counter the effect of the front ring to contract the rear ring in size and prevent leapfrogging. Interestingly, the vortex shedding from the rear ring occurs at  $L/D = 1.5$ , much smaller than the formation number of the isolated vortex ring, around 4 for circular rings generated by a similar piston–cylinder apparatus (Gharib *et al* 1998). A detailed analysis of the dynamics of ring formation with the presence of a front ring is beyond the scope of this research and is the subject of an ongoing study.

The core radius to the toroidal radius ratio  $\alpha$  also plays an important role in the leapfrogging process. For the experiments presented above, the rings are of  $\alpha = 0.41$ . To study the influence of the ring core size on the leapfrogging process, rings with a smaller  $\alpha = 0.29$  are generated. Leapfrogging is observed for these rings with smaller cores. The ring circulations and the axial and radial separations are shown in figure 8. The ring formation processes are similar to that of rings of larger cores. However, there is no shedding of vorticity from the rear ring, because the rear ring experiences less elongation. The front ring, with

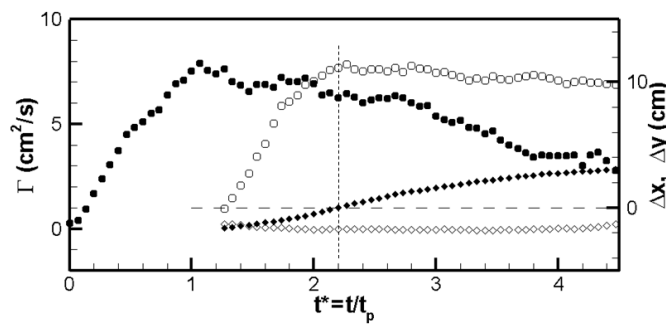


**Figure 8.** Temporal evolution of circulation of the first ring ( $\Gamma_1$ , filled circles) and the second ring generated ( $\Gamma_2$ , open circles) for leapfrogging of rings with smaller cores of  $\alpha = 0.29$ . Also shown are  $\Delta x$  (filled diamonds) and  $\Delta r$  (open diamonds), the separations between peak vorticity locations of two cores in axial and radial directions, plotted to the vertical axis on the right. Vertical dashed lines indicate time instants when  $\Delta x = 0$ . Measurements of  $\Gamma$  begin at  $t^* = 0$ , when the piston starts the first pulse.

a smaller circulation, induces less shear and less elongation of the rear ring. The smaller size of the rear ring core also makes it less subject to deformation. During leapfrogging, the circulation of the front ring decreases due to large dissipation of the small core. The smaller shear induced by the front ring and the smaller core size of the rear ring make the core of the rear ring much less axis touching. Therefore, compared with rings with larger cores in figure 5, there is only a much smaller decrease of circulation for the rear ring, largely due to vorticity dissipation. Vortex rings with an even larger core of  $\alpha = 0.78$  are also studied. However, rings with such large cores merge instead of leapfrogging. Nonetheless, the smaller the ring cores, measured by the core radius to the toroidal radius ratio, the less the ring circulation decreases due to axis touching in the leapfrogging process.

## Acknowledgments

The authors would like to acknowledge the funding from National Science Foundation Grant 1228121 (JP).

## References

- Batchelor G K 1967 *An Introduction to Fluid Dynamics* (Cambridge: Cambridge University Press)
- Gharib M, Rambod E and Shariff K 1998 A universal time scale for vortex ring formation *J. Fluid Mech.* **360** 121–40
- Helmholtz H 1858 Über Integrale der hydrodynamischen Gleichungen, welche den Wirbelbewegungen entsprechen *J. Reine Angew. Math.* **1858** 25–55
- Lamb H 1895 *Hydrodynamics* (Cambridge: Cambridge University Press)
- Lim T T 1997 A note on the leapfrogging between two coaxial vortex rings at low Reynolds number *Phys. Fluids* **9** 239–41
- Mariani R and Kontis K 2010 Experimental studies on coaxial vortex loops *Phys. Fluids* **22** 126102
- Maxworthy T 1972 The structure and stability of vortex rings *J. Fluid Mech.* **51** 15–32
- Maxworthy T 1979 Comments on ‘Preliminary study of mutual slip-through of a pair of vortices’ *Phys. Fluids* **22** 200
- Meleshko V V 2010 Coaxial axisymmetric vortex rings: 150 years after Helmholtz *Theor. Comput. Fluid Dyn.* **24** 403–31
- Oshima Y 1978 The game of passing-through of a pair of vortex rings *J. Phys. Soc. Japan* **45** 660–4
- Oshima Y, Kambe T and Asaka S 1975 Interaction of two vortex rings moving along a common axis of symmetry *J. Phys. Soc. Japan* **38** 1159–66

- Shariff K, Leonard A and Ferziger J H 1989 Dynamics of a class of vortex rings *NASA Technical Memorandum* 102257
- Weigand A and Gharib M 1994 On the decay of a turbulent vortex ring *Phys. Fluids* **6** 3806
- Willert C E and Gharib M 1991 Digital particle image velocimetry *Exp. Fluids* **10** 181–93
- Yamada H and Matsui T 1978 Preliminary study of mutual slip-through of a pair of vortices *Phys. Fluids* **21** 292